Detection of Long-Duration Narrowband Processes

ZHEN WANG

PETER WILLETT, Senior Member, IEEE
University of Connecticut

ROY STREIT
Naval Undersea Warfare Center

Detecting long, weak signals that are narrowband but of unknown frequency structure is an important signal processing challenge, with many applications in remote sensing and process monitoring. An *ad hoc* scheme is developed. Its stages include the discrete Fourier transform (DFT), a multiresolution decomposition in the frequency domain, and a generalized likelihood ratio test (GLRT). The computational load is light, and the performance is remarkably good. This is so not just in the original narrowband situation, but also, due to an inherent adaptivity to the data, in the detection of signals that are relatively broadband in nature. Generalizations are given to constant false alarm rate (CFAR) operation in both prewhitened and unwhitened cases, and to the detection of multiband signals. As regards the last, it is discovered that there is little loss from overestimating the number of bands.

Manuscript reveived December 27, 2000; revised June 27, 2001; released for publication July 18, 2001.

IEEE Log No. T-AES/38/1/02585.

Refereeing of this contribution was handled by J. A. Tague.

This research was supported by NUWC through Contracts N66604-99-1-5021 and N66604-01-1-1125, and by ONR through Contract N00014-98-1-0049.

Authors' addresses: Z. Wang and P. Willett, U-157, University of Connecticut, Storrs, CT 06269-3157, E-mail: (willett@engr.uconn.edu); R. Streit, Naval Undersea Warfare Center, Newport, RI 02841.

I. INTRODUCTION

A. Observation Models

In this paper we are concerned with the detection of quiet narrowband signals. More specifically, we assume that these signals are: 1) extremely weak, with a signal-to-noise ratio (SNR) of −20 dB or below on a per-sample basis, 2) moderately long, of the order of minutes or tens of minutes, and 3) narrowband but not tonal, with, for example, a bandwidth of a few tens of Hz at a sampling rate of a few kHz.

Such signals can arise from a variety of acoustic sources, and detecting them is an important problem in signal processing. As regards the assumption that the signal is narrowband, note that this bandwidth is not known, although it can be assumed not to vary with respect to time. Thus a detector "tuned" for a bandwidth of 10 Hz may perform poorly when in truth the bandwidth is 30 Hz. *Our goal is to establish a detection structure which can take advantage of a narrowband nature, yet is robust when the bandwidth increases.*

There are several possible models for the signals of interest. One is that of a *harmonic set*:

$$x_n = \sum_{k=1}^{K} A_k \exp(j2\pi\alpha_k f_n n) + \nu_n \tag{1}$$

in which $\{x_n\}$ denotes the observations process and ν_n is an additive noise process, assumed white and complex Gaussian, and $n \in \{1,N\}$. Here there are a number K of sinusoids that share a common frequency-modulation process $\{f_n\}$, assumed to be slowly varying; but each complex sinusoid is multiplied by its own complex amplitude A_k and has its own harmonic number α_k, which are not necessarily integral. A second model

$$x_n = \left[\sum_{k=1}^{K} A_k \exp(j2\pi\beta_k n)\right] \exp(j2\pi f_n n) + \nu_n \tag{2}$$

in which a set of low-frequency tones is mixed with a higher frequency carrier may still be termed a harmonic set, but differs from (1) in the nature of the coherence of the harmonic processes. We also propose a third model

$$x_n = \xi_n \star h_n + \nu_n \tag{3}$$

in which $\{\xi_n\}$ is a complex white Gaussian random process, $\star$ denotes convolution, and $\{h_n\}$ the impulse response to a narrowband filter. In all the above models the parameter sets (amplitudes, modulation processes, harmonic numbers) are unknown, although there is some constraint in terms of an assumed narrowband nature. In each case above the *null* hypothesis to be tested against is

$$x_n = \nu_n \tag{4}$$

that the observations are simply white and complex Gaussian. Models other than the above are possible: for example, the fixed amplitudes $\{A_k\}$ in (1) and (2) could be made to vary with time.

B. Ramifications of Model Choice

Because each has unknown parameters, the hypothesis test under each of models (1), (2), and (3) is *composite* and one must use either a generalized likelihood ratio (GLR) [7] or some *ad hoc* scheme.

Harmonic Set Models for the Signal: If one of models (1) or (2) is true, then it is very appropriate to consider an estimator/detector structure. That is, according to the GLR formulation, the amplitudes $\{A_k\}$, basic frequency modulation $\{f_n\}$, and either harmonic numbers $\{\alpha_k\}$ or frequencies $\{\beta_k\}$ must first be estimated from the data. These estimates are then used to form a synthetic signal $\{\tilde{s}_n\}$ (this is the observations model excluding the noise in (1) or (2) with the parameter estimates substituted) and the appropriate test is the comparison of

$$T_{\text{GLR}} = \sum_{n=1}^{N} \Re\{\tilde{s}_n^* x_n\} \tag{5}$$

to a threshold. Unfortunately such parameter estimation routines are very difficult to derive and even more problematic to make converge at low SNRs. Direct-estimation techniques such as [4, 20] would be useful in the absence of appreciable frequency modulation, but are not suited to the situation here. This is also true of the higher order spectral approaches in [1, 20] which rely on phase-coherence between tonal components. The extended Kalman filter (EKF) in [14] is more appropriate, but in common with many EKF applications depends on SNR for its performance. The adaptive notch/comb filter ideas in [9] work reasonably well at low SNR values, but are not compatible with closely-spaced tones. Finally, the expectation-maximization (EM) approach in [8] does appear to work well even down to very low SNR settings, and indeed may eventually be found to be the method of choice; but it is slow, and in any case is not yet ready to be applied to detection.

Filter Model for the Signal: If there is adherence to the signal model (3), of white noise through a narrowband filter, then the key is to estimate that filter, or at least the band of occupancy. Once this is done, substitution of this to a GLR structure is straightforward, and the resulting test is for energy in the "suspicious" band. From an algorithmic perspective it is clearly far easier to estimate parameters under this model, since it amounts to spectral estimation.

Does it Matter?: We have proposed a number of parallel models for the signal to be detected. Clearly some model must be true; the problem is that it is not obvious which. Now, it may be appealing from physical considerations to opt for the more complicated models (1) or (2): all evidence may suggest that the signal, if it exists, should be composed of a group of closely-spaced tones with related modulation. We shall see in Appendix A, however, that as regards *detection* it is not of concern which model is true. It is complicated and problematic to estimate the signals in harmonic set models (1) or (2); but even if one could do it perfectly, one gains essentially nothing as compared to filter model (3). The upshot is that in the remainder of this report we shall assume that the signal is generated according to model (3), the result of white noise being passed through an unknown narrowband (or multiband) filter.

Under model (3) one can propose to use the GLR techniques of [3] based on the discrete Fourier transform (DFT); unfortunately these techniques make little use of the assumed narrowband structure unless a great many parallel GLRs are to be used. A segment of the aggregate spectrum (magnitude-square DFT for the entire length-N signal) for a typical signal is shown in Fig. 14; there are elevated spectral values near the band of occupancy, although at such low SNR values the effect is not marked. Approaches based on order statistics in the spectral domain might be considered, therefore, inappropriate, as indeed we have found them to be.

A more promising approach is the power-law idea of Nuttall [11]; this detector works reasonably well and we use it as a benchmark, but in fact the margin between that and what we propose is considerable. It is reasonable to model the spectrum parametrically, for example via autoregressive means (e.g. [15]) or others such as the Gaussian-primitives in [17]. At low SNRs the convergence of these schemes tends to be poor. The idea of a parametric frequency-domain model is appealing, and in fact that is what we propose. One approach to this is to assume that the spectrum is in fact *piecewise constant*, meaning that there are certain bands of frequency that contain signal energy. The estimation of this piecewise constant function amounts to segmentation, and the most efficient optimal approach to this is based on dynamic programming (DP). We test this, and find that its performance is very good, but that its numerical load is uncomfortably high. What we concentrate on, therefore, is an approximate technique for estimation of the spectrum as a piecewise constant process; our result is ad hoc, but its performance is remarkable.

In Section II we describe the model of our problem, derive the generalized likelihood ratio test (GLRT) based on DP, and introduce the Bartlett and power-law detectors. Our detection structure is described in Section III. Specifically we transform

the data to the frequency domain and use a GLR structure. We then discuss the means of forming this GLR, which is seen to depend on a multiresolution decomposition in the frequency domain—we warn the reader at this point that the technique is logical but *ad hoc*. The new detector structure estimates both signal and noise levels, and hence the extension to constant false-alarm rate (CFAR) operation reported in Section IV is natural. An extension to multiband signals is a similarly small modification, and we report on that also in Section IV. It is seen that the performance loss from the relaxed assumption that there can be several bands is minor even when there is only one band, and hence for robustness we recommend use of the multiband structure. The CFAR operation above allows an unknown background noise level, but requires that the background be white. Thus, in an effort to offer a detection scheme which is usable "off-the-shelf," we develop the corresponding detector for the nonwhite-CFAR case, in which normalization is performed on a frequency-by-frequency basis. Then in Section V we show the performance of the new detector, compared via simulation. It turns out that the structure performs admirably when the signal is narrowband, as was our intention; but the performance even for more broadband signals is similarly good. We give concluding remarks in Section VI, and, as mentioned earlier, we confirm in Appendix A our earlier contention that assumption of model (1), (2), or (3) is for the purpose of detection irrelevant.

II. PROBLEM DESCRIPTION AND ALTERNATIVE DETECTORS

A. Modeling

The problem considered here is of detection of long-duration bandpass signals, whose energy is known to be contained in contiguous frequency observations—at least over multiple fast Fourier transform (FFT) bins—but knowledge about *which* frequency band is not available. As usual, white Gaussian noise is assumed, and the model corresponds to (3). Since the frequency behavior is unknown, the hypotheses (signal-absent and signal-present) to be tested are composite. However, as there is an assumption of *narrowband*ness, or of frequency contiguity, the magnitude-squared FFT is taken on the time-domain observations, and we proceed in the frequency domain.

As shown in Fig. 1, we write in a matrix a block of NL time-domain observations as $\mathbf{x} = (\mathbf{x}_1, \mathbf{x}_2, \ldots, \mathbf{x}_L)$, where $\mathbf{x}_m$ is a column vector of dimension N whose kth element is the time sample of index $(m-1)L + k$. Each column is immediately transformed to its magnitude-squared frequency domain equivalent $\mathbf{X}_m$, and recorded as $\mathbf{X} = (\mathbf{X}_1, \mathbf{X}_2, \ldots, \mathbf{X}_L)$. It is assumed that X_{jm}s are independent.[1]

The probability density function (pdf) of the jth element of $\mathbf{X}_m$, $m = 1,2,\ldots,L$, has the form

$$f(X_{jm}) = \frac{1}{\beta_j}\exp\left(\frac{-X_{jm}}{\beta_j}\right)u(X_{jm}) \tag{6}$$

where $u(\cdot)$ denotes the step function. More specifically, the pdf of the X_{jm}, $j = 1,2,\ldots,N$ and $m = 1,2,\ldots,L$, under hypothesis H_0 follows an independent identically distributed (IID) distribution where all β_js take the constant value $\mu_{0,0}$, usually set to unity for convenience. On the other hand, when a signal is present, the density of X_{jm} has parameter $\beta_j = \mu_{1,1}$ for $j = k_1, k_1+1, \ldots, k_2$ and $m = 1,2,\ldots,L$, where $\mu_{1,1} > \mu_{0,0}$, and k_1 to k_2 are signal-occupying DFT bins. The signal strength $\mu_{1,1}$ and band limits k_1 and k_2 are unknown parameters.

Presented in a hypotheses-testing framework and with $\mu_{0,0} = 1$, we have the model

$$\mathbf{H}_0: \quad f_\theta(\mathbf{X}) = \prod_{m=1}^{L}\prod_{j=1}^{N}\exp(-X_{jm})u(X_{jm}) \tag{7}$$

$$\mathbf{H}_1: \quad f_\theta(\mathbf{X}) = \left[\prod_{m=1}^{L}\prod_{j\in\mathcal{S}}\frac{\exp(-X_{jm}/\mu_{1,1})}{\mu_{1,1}} \times \prod_{j\notin\mathcal{S}}\exp(-X_{jm})\right]u(X_{jm}) \tag{8}$$

where $\mathcal{S}$ indicates the (unknown) subset $\{k_1, k_1+1, \ldots, k_2\}$ in which signal energy is to be found and $\theta = \{\mu_{1,1}, k_1, k_2\}$ are the parameters. The model can be equivalently presented as

$$\begin{aligned}\mathbf{H}_0: &\quad \beta_j = 1, \qquad 1 \le j \le N \\ \mathbf{H}_1: &\quad \beta_j = \begin{cases}\mu_{1,1}, & k_1 \le j \le k_2 \\ 1, & \text{else}\end{cases}\end{aligned} \tag{9}$$

with reference to (6).

B. Bartlett Approach

Since our motivating signal is of a tone-cluster with a quite narrow bandwidth, an appropriate contender is the Bartlett scheme [15] favored in [22] for the detection of a single tone in white Gaussian noise. This approach can be summarized as: divide the time-domain observation $\mathbf{x}$ into K nonoverlapping segments each of length M, compute the periodogram (magnitude-square DFT) for each

[1]This assumption of independence is in practice only approximate. In what follows, for analysis we use the assumption; our simulations are based on time domain signals, and naturally there is a truer representation of the dependency structure.

segment, average these across segments to form the Bartlett periodogram, and finally use as a test statistic the largest value in this. It is seen that this approach is very good when the signal is indeed tonal (or at least extremely narrowband), and its performance is essentially as good as that of the new detector. However, as the bandwidth of the signal grows, the margin in performance between these detectors becomes considerable.

C. Power-Law Detector

Nuttall's power-law detector [11, 13] has attracted considerable recent attention due to its simple implementation and good performance. In the multiblock case it is formed as

$$T_{\mathrm{PL}} = \sum_{m=1}^{L}\sum_{j=1}^{N} X_{jm}^{\nu}. \tag{10}$$

The power-law detector performs essentially optimally, assuming that signal-present bins are uniformly distributed; the idea is similar to that in [2] for time-domain data. However, many signals of interest tend to focus their energy in a band. Taking advantage of this tendency simply by combining contiguous bins, several new power-law detectors were developed in [18]. The detectors show exceptional performance and are easy to implement. For instance, the detector combining 2 contiguous FFT bins is simply formed as

$$T_{f2} = \sum_{m=1}^{L}\sum_{j=1}^{N} (X_{j,m} + X_{j+1,m})^{\nu}. \tag{11}$$

Similarly, by combining 3 contiguous FFT bins, we can write T_{f3}. CFAR versions of these statistics, and similar statistics based on an initial wavelet decomposition rather than the DFT, are also developed.

D. Generalized Likelihood Ratio Test

In hypothesis testing with unknown parameters, a typical approach is to replace the unknown parameters by their maximum likelihood estimates (MLEs), termed the GLRT [6, 7]. Based on the model of (7), the GLR is

$$T_{\mathrm{GLR}}(\mathbf{X}) = \frac{\max_{\theta\in\Theta_1}\{f_\theta(\mathbf{X})\}}{f_{\theta_0}(\mathbf{X})} \tag{12}$$

where θ_0 is the known parameter set under H_0 and the set Θ_1 includes all the possible choices of parameter θ under H_1.

The GLRT usually involves enumeration of all possible parameter values when the model is discrete, and hence the computational cost can be high. Fortunately, the model (9) suggests an efficient DP approach [10], since the problem can be regarded as one of segmentation. This is presented in Appendix B. The DP approach results in a GLR T_{DP}, and its performance in terms of detection can therefore be regarded as optimal. However, despite its efficiency as compared with a less clever search, its computational load can still be prohibitive, especially for large data records.

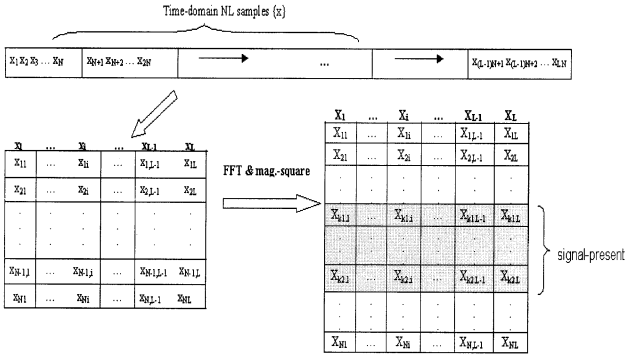

Fig. 1. Illustration of data preprocessing. Long data record is reshaped to a matrix, and DFT is applied columnwise.

Our goal is to find a quick detection structure with slight performance loss as compared with the DP approach; we derive such a one based on the multiresolution decomposition in Section III.

III. NEW DETECTOR

Due to the assumption of complex white Gaussian noise and the frequency contiguity of signals of interest, the vector of $\{\beta_j\}$s is piecewise constant, meaning notionally that β_j is either in a spectral region of noise power only or a region with a signal contribution as well. This localization of energy suggests that a multiresolution decomposition may be appropriate, and motivates us to estimate the $\{\beta_j\}$s using wavelet coefficients *in the frequency domain*. There are many different wavelet families, and each has its proponents [16]; here only the Haar wavelet, the first and simplest, is used due to its easy implementation.

It is assumed that the data has been preprocessed as in Fig. 1. The steps used to derive the estimates for the βs are presented here, and reference to the accompanying Fig. 2 may be helpful.

1) *Coarsely estimate the βs by averaging across time.* The spectral behavior of an observation is faithfully represented by the N βs. It is assumed that for the entire block of observation the jth frequency bin maintains a mean energy level β_j for each of the L blocks of N data. In the unconstrained situation (meaning that there is no attempt to exploit frequency-contiguity or its piecewise-constant character) the MLE of β can be easily obtained as

$$\beta_j^{\mathrm{UML}} = \frac{\sum_{m=1}^{L} X_{jm}}{L} \tag{13}$$

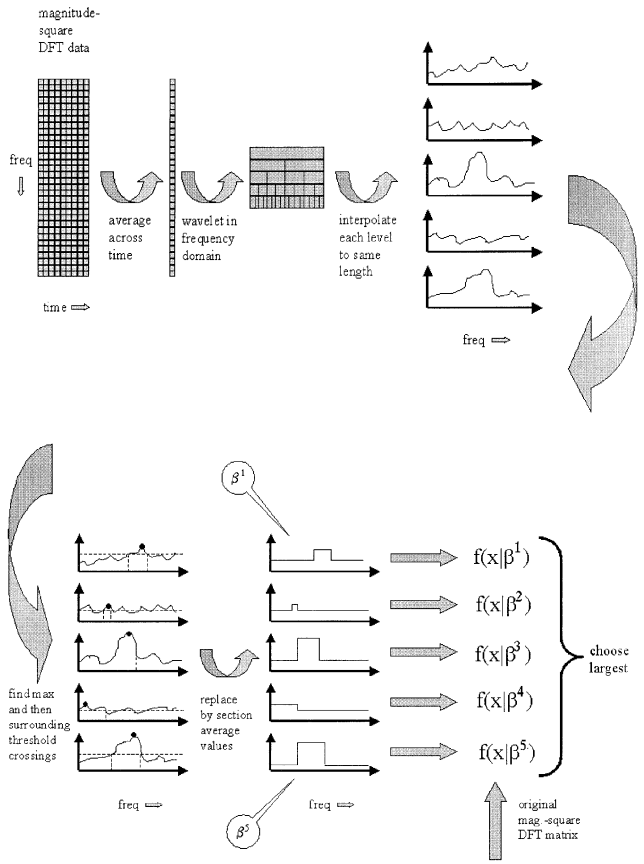

Fig. 2. Illustration of entire estimation/GLRT processing flow. Data is first arranged in magnitude-square DFT matrix according to Fig. 1, in the upper left. Wavelet decomposition is suggested in Fig. 3. Interpolation phase is performed according to Fig. 4.

for $j = 1,2,\ldots,N$, the superscript UML denotes unconstrained ML estimation.

2) *Perform a multi-resolution decomposition on* $\{\beta_j^{\mathrm{UML}}\}$. With the vector $\{\beta_j^{\mathrm{UML}}\}$ as the input signal, the wavelet decomposition process operates, generating lower resolution coefficients having only half the length due to downsampling, as shown in Fig. 3. We denote the kth element of the ith-level decomposition as $cA_i(k)$. Note that the maximum

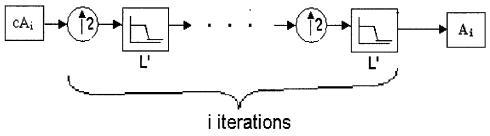

Fig. 4. Reconstructing ith level approximation A_i from coefficient vector cA_i. L' is reconstruction low-pass filter associated with decomposition filters in Fig. 3.

number of levels is $\log_2(N)$, where N is the length of the original signal, and as is well known, the computational load of a wavelet decomposition is comparatively light.

3) *Interpolate each scale level to the same length.* Since we aim to reveal the overall trend of the $\{\beta_j^{\mathrm{UML}}\}$s, the approximation coefficients $\{cA_i(k)\}$ contain the necessary information. However, cA_i contains only $N/2^i$ elements, and hence it is necessary to reconstruct the approximations A_i, as illustrated in Fig. 4, each having the same length N as the original signal, and presumably recognizable as an approximation of it. As the scale i increases, the resolution decreases, producing an estimate of the unknown trend at a broader scale.

4) *For each scale compute the mean level.* We compute

$$\eta_i = \frac{1}{N}\sum_{k=1}^{N} A_i(k) \tag{14}$$

and this is used as a threshold level to determine the spectral extent of the signal.

5) *For each scale find the region of signal energy.* It is assumed that if the bandwidth of the signal is such that its appearance will be most evident at scale i, then there will be a peak in $\{A_i(k)\}$ around the element corresponding to that frequency band. Discovery of this is a two-stage process.

a) Compute

$$k_i^{\max} = \arg\max_k \{A_i(k)\} \tag{15}$$

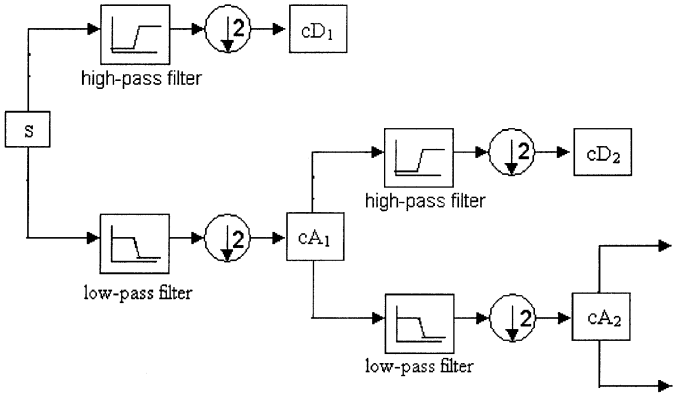

Fig. 3. Multiple-level wavelet decomposition. S means the signal, cA_i indicates approximation coefficients at ith level, cD_i indicates corresponding detail coefficients.

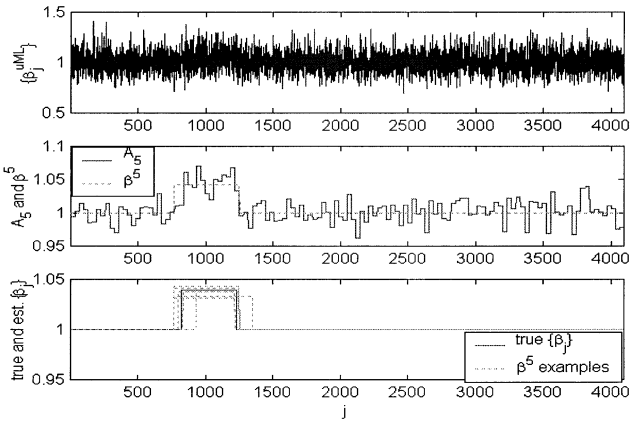

Fig. 5. Illustration of process of estimating $\{\beta_j\}$ from ith level approximation A_i. In this example, $N = 4096$, $L = 100$, scale level is $i = 7$, signal energy is with frequency band [0.2,0.3] (corresponding to DFT bins [820,1229]) and aggregate $SNR = 1600$. Upper 2 plots show one specific example; bottom plot presents estimates of 10 observations by ensemble of dotted lines for same signal model and at same scale resolution level 5.

which is the location (in frequency, with respect to Fig. 2) at which the ith-scale decomposition reaches its maximum value.

b) Find the left and right "shoulders" of the peak according to

$$\begin{aligned} k_1^i &= \max\{k : k < k_i^{\max} \text{ and } A_i(k) < \eta_i\} \\ k_2^i &= \min\{k : k > k_i^{\max} \text{ and } A_i(k) < \eta_i\}. \end{aligned} \tag{16}$$

For scale i a candidate signal band is thus that of frequencies between $2\pi k_1^i/N$ and $2\pi k_2^i/N$ rad/s.

6) *Estimate the signal energy profile for each scale.* We form $\{\beta_j^i\}$, the estimate of the vector $\{\beta_j\}$ using A_i, using the constraint that under H_1, $\beta_j = \mu_{1,1}$ for $k_1 \le j \le k_2$, and $\beta_j = \mu_{1,0} \equiv 1$ otherwise. The MLE of $\mu_{1,1}$ based on the ith-scale data is thus

$$\hat{\mu}_{1,1}^i = \frac{1}{k_2^i - k_1^i + 1} \sum_{j=k_1^i}^{k_2^i} A_i(j). \tag{17}$$

The process up to this point is illustrated in Fig. 5, where $N = 4096$, $L = 100$, the scale level $i = 5$, and the signal energy is within the (relatively large) frequency band [0.2,0.3]. It is clear that the resulting $\{\beta_j^5\}$ based on the above process gives the appropriate estimation to $\{\beta_j\}$ although the initial estimate $\{\beta_j^{\text{UML}}\}$ is far from correct. Note also the repeatability of the procedure over several examples.

7) *Calculate of the GLR statistics based on each scale.* Each scale of the multiresolution analysis is a candidate to represent the "real" band of signal energy, and each must be interrogated. We thus compute the GLR for scale i as

$$T_G^i = \prod_{m=1}^{L} \prod_{j=1}^{N} \frac{1}{\beta_j^i} e^{X_{jm}(1-1/\beta_j^i)} \tag{18}$$

according to (7); or equivalently

$$T_g^i = \left[\sum_{m=1}^{L} \sum_{j=k_1^i}^{k_2^i} X_{jm}(1 - 1/\hat{\mu}_{1,1}^i) \right] - L(k_2^i - k_1^i + 1)\ln(\hat{\mu}_{1,1}^i) \tag{19}$$

which takes advantage of the monotonicity of log function and the bilevel nature of β_j^i.

8) *Find the overall GLR by maximizing over the GLRs at the various scales.* That is,

$$T_G = \max_i \{T_G^i\} \tag{20}$$

is the overall test statistic.

The above procedure is quite ad hoc; but it works very well and robustly, both for narrowband and for broadband signals, and down to very low SNR values. An additional feature is that its computation is relatively light.

IV. EXTENSIONS OF NEW DETECTOR

A. Extension to Signals with Multiple Bands

The detection procedure developed here was designed to discover narrowband signals. In some cases, however, the signal of interest may, due to nonlinearities in its mechanism of origin, or due to the difference in relative Doppler shifts from multipath arrivals, be of a multiband nature. Further, in such cases, it is not reasonable to specify that the signal level in each band be identical. Fortunately, it is straightforward to modify the detector to accommodate multiple signal bands. We assume that the number of signal-occupied frequency bands is known to be M; model (9) now becomes

$$\begin{aligned} \mathbf{H}_0: &\quad \beta_j = \mu_{0,0} = 1 \\ \mathbf{H}_1: &\quad \beta_j = \begin{cases} \mu_{1,p} & k_1(p) \le j \le k_2(p) \\ & \text{and} \quad p = 1,2,\ldots,M \\ \mu_{1,0} = 1 & \text{else} \end{cases} \end{aligned} \tag{21}$$

where $[k_1(p),k_2(p)]$ indicates the location of the pth band with energy level $\mu_{1,p}$.

The procedure is similar to the basic (single-band) one in Section III; the difference is that band-finding process should be iterated M times at each scale level. Specifically, Steps 5–6 from Section III are iterated, with initial $p = 1$, and p incremented each time. Steps 5 through 7 become:

5) *(Multiband). For each scale find the region of signal energy.*

a) Compute

$$k_i^{\max}(p) = \arg\max_k \{A_i(k)\} \tag{22}$$

which is the location (in frequency, with respect to Fig. 2) at which the ith-scale decomposition reaches its maximum value.

b) Find the left and right "shoulders" of the peak according to

$$\begin{aligned} k_1^i(p) &= \max\{k : k < k_i^{\max}(p) \text{ and } A_i(k) < \eta_i\} \\ k_2^i(p) &= \min\{k : k > k_i^{\max}(p) \text{ and } A_i(k) < \eta_i\}. \end{aligned} \tag{23}$$

6) *(Multiband). Estimate the signal energy profile for each scale.* The MLE of $\mu_{1,1}(p)$ based on the ith-scale data is thus

$$\hat{\mu}_{1,p}^i = \frac{1}{k_2^i(p) - k_1^i(p) + 1} \sum_{j=k_1^i(p)}^{k_2^i(p)} A_i(j). \tag{24}$$

In order that the next iteration be initialized, remove the currently found band from consideration according to

$$A_i(j) = \begin{cases} \eta_i & k_1^i(p) \le j \le k_2^i(p) \\ A_i(j) & \text{else} \end{cases} \tag{25}$$

meaning that the band with the previously discovered "peak" becomes flat. Then increment p: if $p \le M$, go back to Step 5, and otherwise proceed to Step 7.

7) *(Multiband). Calculation of the GLR statistics based on each scale.* We compute

$$\begin{aligned} T_g^i = \sum_{p=1}^{M} \Bigg[& \sum_{m=1}^{L} \sum_{j=k_1^i(p)}^{k_2^i(p)} X_{jm}(1 - 1/\mu_{1,p}^i) \\ & - L(k_2^i(p) - k_1^i(p) + 1)\ln(\hat{\mu}_{1,p}^i) \Bigg]. \end{aligned} \tag{26}$$

B. Extension to CFAR Operation for Prewhitened Data

The GLR detector in Section III assumes that the noise level is known ($\mu_{0,0} = 1$), and is thus open to criticism in its normalization needs. Here we consider the case where $\mu_{0,0}$ is unknown and also requires estimation. The model (9) becomes

$$\begin{aligned} \mathbf{H}_0 &: \quad \beta_j = \mu_{0,0}, \quad j = 1,2,\ldots,N \\ \mathbf{H}_1 &: \quad \beta_j = \begin{cases} \mu_{1,1}, & k_1 \le j \le k_2 \\ \mu_{1,0}, & \text{else} \end{cases} \end{aligned} \tag{27}$$

where $\{\mu_{0,0}, \mu_{1,0}, \mu_{1,1}, k_1, k_2\}$ indicate the parameters to be estimated.

In fact, the modification is quite straightforward. Step 6 of the procedure from Section III now uses

$$\begin{aligned} \hat{\mu}_{0,0}^i &= \frac{1}{N} \sum_{j=1}^{N} A_i(j) \\ \hat{\mu}_{1,0}^i &= \frac{1}{N - (k_2^i - k_1^i + 1)} \sum_{j \notin \{k_1^i, k_2^i\}} A_i(j) \\ \hat{\mu}_{1,1}^i &= \frac{1}{k_2^i - k_1^i + 1} \sum_{j \in \{k_1^i, k_2^i\}} A_i(j) \end{aligned} \tag{28}$$

and the GLR in Step 7 becomes

$$\begin{aligned} T_g^i = & \left[\sum_{m=1}^{L} \sum_{j \notin \{k_1^i, k_2^i\}} X_{jm}(1/\hat{\mu}_{0,0}^i - 1/\hat{\mu}_{1,0}^i) \right] \\ & + \left[\sum_{m=1}^{L} \sum_{j \in \{k_1^i, k_2^i\}} X_{jm}(1/\hat{\mu}_{0,0}^i - 1/\hat{\mu}_{1,1}^i) \right] \\ & + LN\ln(\hat{\mu}_{0,0}^i) - L(k_2^i - k_1^i + 1)\ln(\hat{\mu}_{1,1}^i) \\ & - L(N - [k_2^i - k_1^i + 1])\ln(\hat{\mu}_{1,0}^i). \end{aligned} \tag{29}$$

This detector is naturally CFAR.

C. Extension to CFAR Operation for Nonwhite Data

The previous Section IVB discussed the case that the noise process was known to be white, but was of unknown level. In that case estimation of the noise level ($\mu_{0,0}$ and/or $\mu_{1,0}$) was a natural extension to the procedure. The detector developed in this section operates on data which has arbitrary spectrum. Naturally there must be a segment of noise-only "training" data on which the spectrum can be estimated; in fact we use a direct normalization that alters the exponential character of the data and requires that an alternative nonlinear GLR statistic be used. This form of the detector is perhaps of the greatest practical use, but the stationarity assumption is strong considering that the detection records are assumed to be lengthy.

1) *Problem Description and Modeling*: The focus of this section is to detect long-duration narrowband signal buried in colored noise with unknown but stationary spectrum. Similar frequency-domain preprocessing as in Section III is used, and we then record the data as $\mathbf{X} = \{X_1, X_2, \ldots, X_{L^{\text{norm}}}, \ldots, X_L\}$, where X_{ji}s are assumed independent, and $\{X_1, \ldots, X_{L^{\text{norm}}}\}$ are known to be noise-only samples.[2] The jth element of X_m, $m = 1,2,\ldots,L^{\text{norm}}$ has the pdf

$$f(X_{jm}) = \frac{1}{\alpha_j} \exp\left(\frac{-X_{jm}}{\alpha_j}\right) u(X_{jm}) \tag{30}$$

where the $\{\alpha_j\}$ are unknown.

Our goal is to test whether the signal is present in the latter $L - L^{\text{norm}}$ snapshots. More specifically, the pdf of X_{jm}, $m = L^{\text{norm}} + 1, \ldots, L$, under hypothesis H_0 follows a distribution identical to X_{jm}, $m = 1, \ldots, L^{\text{norm}}$. On the other hand, when a signal is present, the density of X_{jm}, $L^{\text{norm}} + 1 \le m \le L$, has the form

$$f(X_{jm}) = \frac{1}{\alpha_j \beta_j} \exp\left(\frac{-X_{jm}}{\alpha_j \beta_j}\right) u(X_{jm}) \tag{31}$$

[2]We have written the L^{norm} snapshots of noise-only normalizing data as immediately preceding the data under test. In practice there may be a "guard" band of data separating the two windows.

with $\beta_j = \mu_{1,1} > 1$ for $k_1 \le j \le k_2$, and unity otherwise. The relative signal power $\mu_{1,1}$ and band limits k_1, k_2 are unknown parameters. Overall, we have the model

$$\begin{aligned}
\mathbf{H}_0: \quad f(\mathbf{X}) &= \prod_{m=1}^{L}\prod_{j=1}^{N}\frac{1}{\alpha_j}\exp\left(\frac{-X_{jm}}{\alpha_j}\right)u(X_{jm}) \\
\mathbf{H}_1: \quad f(\mathbf{X}) &= \left[\prod_{m=1}^{L^{\text{norm}}}\prod_{j=1}^{N}\frac{1}{\alpha_j}\exp\left(\frac{-X_{jm}}{\alpha_j}\right)u(X_{jm})\right] \\
&\quad \times\left[\prod_{m=L^{\text{norm}}+1}^{L}\prod_{j\in\mathcal{S}}\frac{\exp\left(\frac{-X_{jm}}{\alpha_j\mu_{1,1}}\right)}{\alpha_j\mu_{1,1}}\right. \\
&\quad \left.\times\prod_{j\notin\mathcal{S}}\frac{1}{\alpha_j}\exp\left(\frac{-X_{jm}}{\alpha_j}\right)\right]u(X_{jm})
\end{aligned} \tag{32}$$

where, as in Section III, $\mathcal{S}$ indicates the (unknown) subset $\{k_1, k_1+1, \ldots, k_2\}$ in which signal energy is to be found.

Since we intend to detect signals irrespective of the spectrum of the background, as represented by $\{\alpha_j\}$, we define the *normalized* observations as

$$z_j = \frac{\frac{1}{L-L^{\text{norm}}}\sum_{m=L^{\text{norm}}+1}^{L}X_{jm}}{\frac{1}{L^{\text{norm}}}\sum_{m=1}^{L^{\text{norm}}}X_{jm}} \tag{33}$$

for $j = 1, \ldots, N$. Under $\mathbf{H}_0$, the z_js follow an IID F-distribution $F(2(L-L^{\text{norm}}), 2L^{\text{norm}})$; when signal energy is present in the jth bin, they become distributed according to a generalized F-density [5]. In either case, the density of z_j is free of α_j. Thus, similar to (32), the following model holds:

$$\begin{aligned}
\mathbf{H}_0: \quad f(\mathbf{z}) &= \prod_{j=1}^{N}\frac{\left(\frac{L-L^{\text{norm}}}{L^{\text{norm}}}\right)^{L-L^{\text{norm}}}}{B(L-L^{\text{norm}}, L^{\text{norm}})}\frac{z_j^{L-L^{\text{norm}}-1}}{\left(1+\frac{L-L^{\text{norm}}}{L^{\text{norm}}}z_j\right)^{L}}u(z_j) \\
\mathbf{H}_1: \quad f(\mathbf{z}) &= \prod_{j\in\mathcal{S}}\frac{\left(\frac{L-L^{\text{norm}}}{L^{\text{norm}}}\right)^{L-L^{\text{norm}}}}{B(L-L^{\text{norm}}, L^{\text{norm}})}\frac{(1/\mu_{1,1})(z_j/\mu_{1,1})^{L-L^{\text{norm}}-1}}{\left(1+\frac{L-L^{\text{norm}}}{L^{\text{norm}}}\frac{z_j}{\mu_{1,1}}\right)^{L}} \\
&\quad \times\prod_{j\notin\mathcal{S}}\frac{\left(\frac{L-L^{\text{norm}}}{L^{\text{norm}}}\right)^{L-L^{\text{norm}}}}{B(L-L^{\text{norm}}, L^{\text{norm}})}\frac{z_j^{L-L^{\text{norm}}-1}}{\left(1+\frac{L-L^{\text{norm}}}{L^{\text{norm}}}z_j\right)^{L}}u(z_j)
\end{aligned} \tag{34}$$

where $\mathcal{S}$ indicates the subset $\{k_1, k_1+1, \ldots, k_2\}$, and $\{\mu_{1,1}, k1, k2\}$ are estimated parameters, and in which $B(\cdot,\cdot)$ denotes the beta function. Therefore, model (9) continues to hold, with reference to (34) now.

2) *Detector*: We assume that normalization of the frequency domain data according to (33) has already occurred. With the $\{z_j\}$ serving as the coarse estimate of βs (Step 1 therefore), a procedure parallel to that in Section III is used to estimate the βs and to test—the only difference is in the seventh step, in which the GLR statistics are calculated.

7) *Calculation of the statistics based on each scale.* According to the new (F-distributed) model we have

$$T_G^i = \prod_{j=1}^{N}\left(\frac{1}{\beta_j^i}\right)^{L-L^{\text{norm}}}\left(\frac{1+(L-L^{\text{norm}})/L^{\text{norm}}z_j}{1+\frac{L-L^{\text{norm}}}{L^{\text{norm}}}\frac{z_j}{\beta_j^i}}\right)^{L} \tag{35}$$

according to (34); or

$$\begin{aligned}
T_g^i = L\left[\sum_{j=k_1^i}^{k_2^i}\left(\log(1+(L-L^{\text{norm}})/L^{\text{norm}}z_j)\right.\right. \\
\left.\left.-\log\left(1+\frac{L-L^{\text{norm}}}{L^{\text{norm}}}\frac{z_j}{\hat{\mu}_{1,1}^i}\right)\right)\right] \\
-(L-L^{\text{norm}})(k_2^i-k_1^i+1)\log(\hat{\mu}_{1,1}^i)
\end{aligned} \tag{36}$$

equivalently.

Note that T_G is clearly CFAR with respect to $\{\alpha_j\}$, representing the colored-noise spectrum. Further, using a derivation similar to that in Section IVA, the above procedure can be easily modified to accommodate multiple signal bands.

V. RESULTS

A. Basic Detector

As is often the case for a GLRT, direct analytical evaluation is infeasible, and consequently our performance analysis is based on simulation. For consistency, in all our simulations, we set $N = 4096$, $L = 100$, corresponding to approximately 68 s of data at a 6 kHz sampling rate. All simulations use the narrowband-signal assumption of (3). Here, four different choices of relative frequency bandwidth, 0.003, 0.01, 0.1 and 0.3, corresponding, respectively, to 18, 60, 600, and 1800 Hz, are explored. Note that the first of these corresponds to the motivating situation of a quite narrow signal bandwidth (each DFT bin corresponds to 1.4 Hz); the detector is seen to perform well in that situation, also to be robust with respect to bandwidth.

We first compare in Fig. 6 the performance of the basic version of the new detector (single band and non-CFAR), from Section III, to the GLRT based on DP (T_{DP}), the power-law detectors of [11] (T_{PL}) and the refined version of it introduced in [18]. The CPU time required for each detector is also shown in Table I. It can be seen that the detector T_{G} shows little

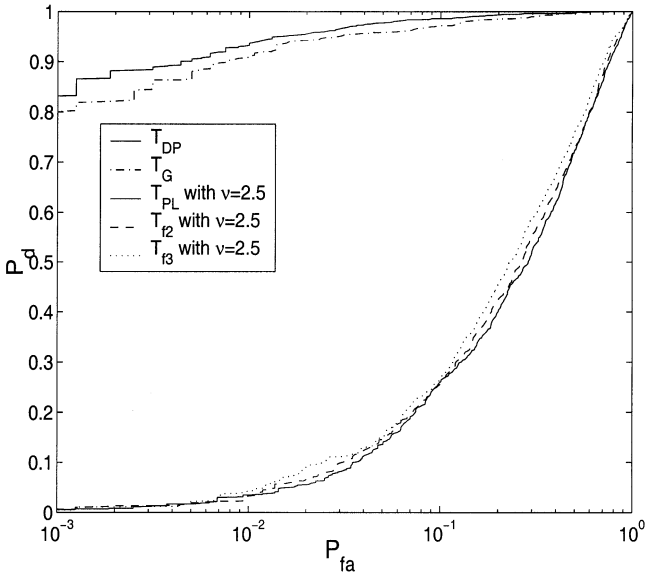

Fig. 6. ROCs of detectors for signal with frequency band [0.3,0.31]. Aggregate $SNR = 400$. T_{DP} represents GLRT based on DP, T_G for our wavelet-based GLR scheme, T_{PL} for basic power-law detectors, T_{f2} and T_{f3} for combining 2 and 3 contiguous FFT bins, respectively.

performance loss compared with the (optimal) T_{DP}, but with remarkably reduced computational needs.

Next, for each bandwidth choice and with fixed $P_{fa} = 10^{-4}$, the performance of detectors is compared and presented versus aggregate SNR, as shown in Fig. 7. Since different exponents (νs) mean different power-law detectors, we show only the performance of the *best* power-law detector in each case and those with $\nu = 2.5$, often considered the best compromise value. Again, it is clear that T_G provides performance close to that of T_{DP} at a far lighter numerical expense. The new detector T_G does require more CPU time than the power-law detector, but there is a considerable performance benefit as compared even to the power-law detectors based on energy contiguity (e.g. (11)). This improvement is most marked for low-bandwidth signals—exactly the sort that provided motivation in the first place—but there is significant outperformance at all bandwidth levels. We also make comparison to the Bartlett scheme using DFTs of length $N = 256$ in Fig. 7. In the first and most narrowband case of Fig. 7(a), to which the Bartlett approach is "tuned," the performances are essentially identical; as the bandwidth increases in Fig. 7(b)–(d) the Bartlett scheme performs increasingly poorly.

TABLE I
CPU Time For Various Detectors

Detector	T_{DP}	T_G	T_{PL}
Mean CPU time (s)	25.0966	0.3843	0.0385

Note: Result is based on 2000 simulation runs. Data length corresponds to approximately 68 s.

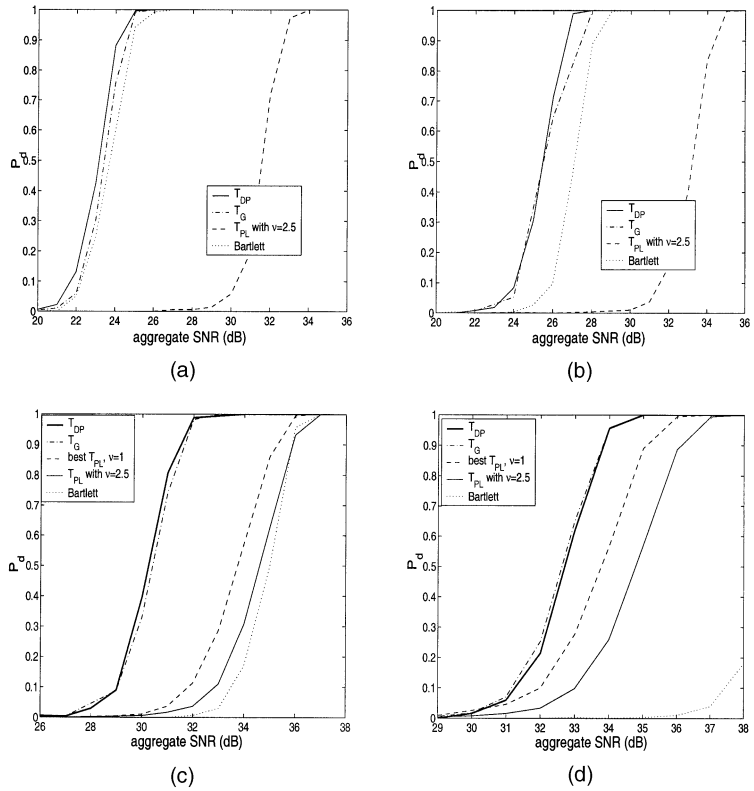

Fig. 7. Detection performance of basic detector T_G (from Section III) for signals with different frequency bands. (a) Frequency band is [0.2,0.203]. (b) Frequency band is [0.3,0.31]. (c) Frequency band is [0.3,0.4]. (d) Frequency band is [0.2,0.5].

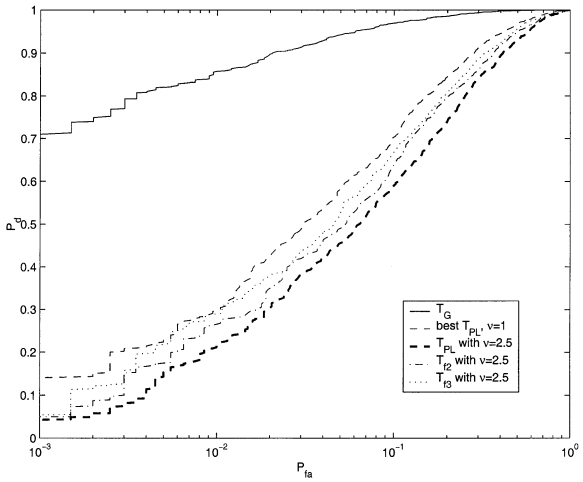

Fig. 8. Detection performance of detector T_G (from Section IVA) for signal with multiple frequency bands. Aggregate $SNR = 1200$, and number of bands M set to 3. Power-law detector with $\nu = 1$ provides best performance.

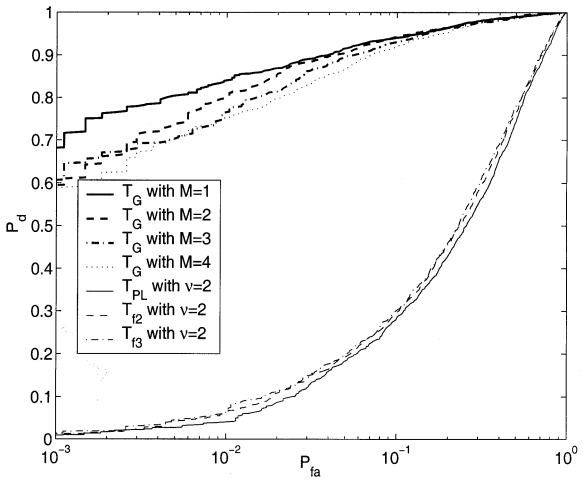

Fig. 9. Detection performance of detector T_G for signal when an incorrect assumption about number of bands M is made. Here the true band is $[0.3, 0.32]$, and aggregate $SNR = 500$. Power-law detector with $\nu = 2$ provides the best performance.

B. Multiple-Band Detector

The performance of the multiband version of the new detector, from Section IVA, is illustrated and compared with the power-law detectors in Fig. 8. Here the aggregate $SNR = 1200$ and the number of bands M set to 3—specifically $[0.2, 0.22]$, $[0.4, 0.45]$ and $[0.6, 0.61]$, with relative amplitude, 1.5, 1 and 1.5, respectively. It can be seen that this scheme works extremely well.

Since the number of frequency bands M is likely to be unknown beforehand, the robustness with respect to an incorrect selection of M is studied in Fig. 9, in which truth is that $M = 1$, with occupied band $[0.3, 0.32]$, and aggregate $SNR = 500$. In Fig. 9 the cases that the *assumed* value is $M = 1, 2, 3$ and 4 are examined separately; apparently there is some loss in overestimating M, but this loss is minor.

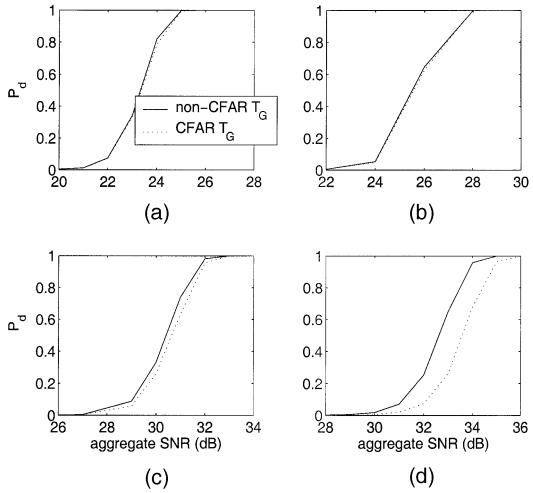

Fig. 10. Detection performance of our CFAR detector for prewhitened signals with different frequency bands. Here T_G represents our wavelet-based GLR scheme. (a) Frequency band is $[0.2, 0.203]$. (b) Frequency band is $[0.3, 0.31]$. (c) Frequency band is $[0.3, 0.4]$. (d) Frequency band is $[0.2, 0.5]$.

C. CFAR Detector for Prewhitened Data

This version of the new detector is that presented in Section IVB. Due to the lack of comparable statistics in this CFAR case, we simply evaluate the CFAR loss in Fig. 10. The loss is very small, less than 1 dB. The tendency of the CFAR loss to increase with increasing signal bandwidth is presumably due to the reduction in the number of samples used to calculate $\hat{\mu}_{1,0}$.

D. General CFAR Detector

This is perhaps the most useful form of the new detector, and refers to that presented in Section IVC. For comparison, we introduce from [18] the corresponding CFAR power-law statistics T_{cpl}, defined as

$$T_{\text{cpl}} = \sum_{j=1}^{N} z_j^{\nu} \tag{37}$$

where ν is a real exponent. By taking advantage of assumed frequency contiguity, we also form the detectors T_{cf2} and T_{cf3}, which combine, respectively, 2 and 3 contiguous DFT bins, as in (11). The detection performance of the new scheme is illustrated and compared with the best CFAR power-law detectors of (37) in Fig. 11 with different choices of relative frequency bandwidth and signal power. In all simulations, we set $N = 4096$, $L^{\text{norm}} = 30$ and $L = 90$. As in the white noise situation there is a significant improvement in detection capability provided by our new wavelet-based GLR detector at all, especially low, bandwidth levels. At low signal bandwidths (0.33% and 1%) the improvement is approximately 4 dB; at moderate bandwidth (10%) the improvement reduces

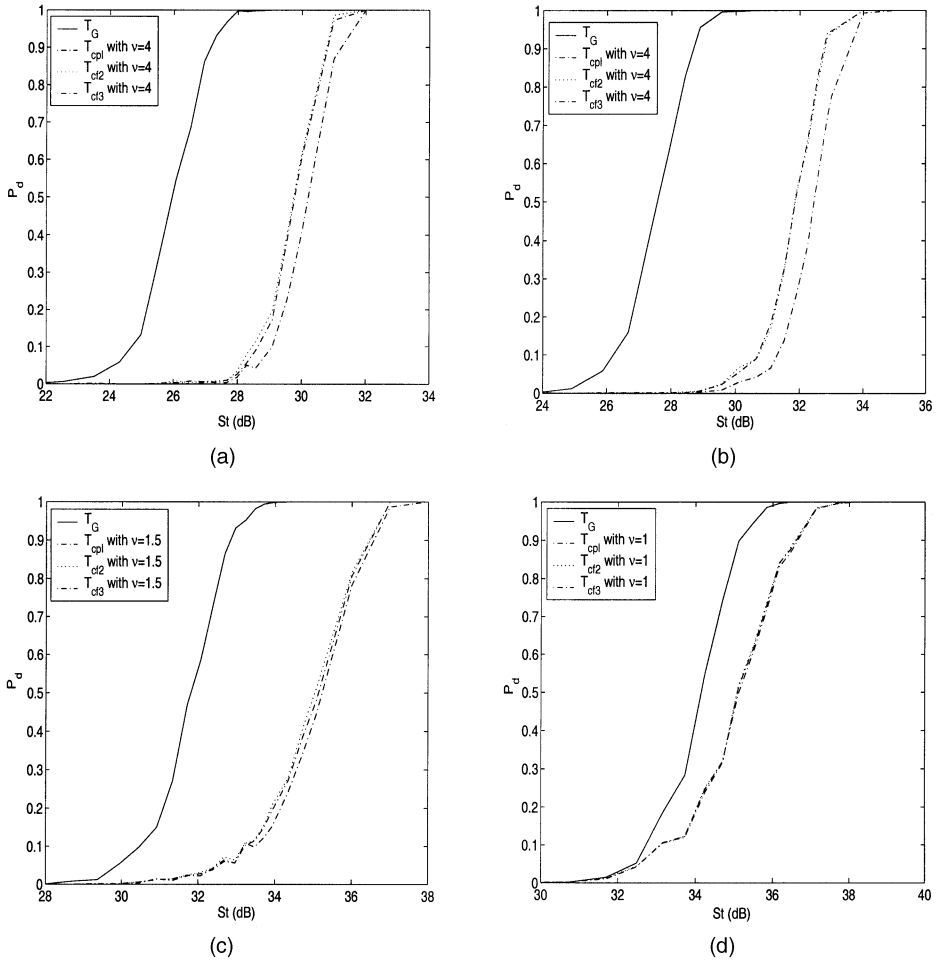

Fig. 11. Detection performance of unwhitened CFAR version of detector T_G (see Section IVC) for signals with different frequency bands. (a) Frequency band is [0.2,0.203]. (b) Frequency band is [0.3,0.31]. (c) Frequency band is [0.3,0.4]. (d) Frequency band is [0.2,0.5]. Comparison is to CFAR versions of power-law detector from [18], in which only the best exponent is shown, and in which both "standard" (T_{cpl}) and frequency-combining (T_{cf2} and T_{cf3}) are shown. Relative aggregate SNR St is defined as $(L - L^{\mathrm{norm}})(k_2 - k_1 + 1)(\mu_{1,1} - 1)$.

to about 2 dB, and even for wideband signals (30%) there is still some performance advantage.

VI. SUMMARY

In this paper we have sought a detector for a signal that is long (minutes), weak (below −20 dB on a per-sample basis) and narrowband (less than 1% of sampling frequency). As regards the last, neither the central frequency nor the bandwidth is known a-priori; further, whether the signal is indeed narrowband, in the sense of adequately modeled by the passage of a white process through a narrowband filter, or whether a deeper model involving a cluster of closely-spaced and commonly-modulated sinusoids is more appropriate, is unknown. (In an Appendix we show that any elaborate modeling of the signal is unrewarding from the detection perspective; even if there were to exist an algorithm that could usefully estimate such a tone-cluster process, there is little improvement in performance relative to the simpler model.)

The paper proceeds to develop a means to detect such signals under the weaker assumption. The scheme is illustrated best in Fig. 2; stages include magnitude-square discrete Fourier transformation, a multiresolution decomposition in the frequency domain with associated interpolation to preserve length, a peak-/band-picking routine at each scale, and formation of a GLR statistic. The scheme is admittedly *ad hoc*; however, its performance is good, and its computational load is comparable to that of the original DFT-step alone. The performance of the resulting scheme is actually *remarkably* good, not just in the motivating situation of a narrowband process, but also in the case of reasonably broadband signals. That is a strength of the approach. The "band" of signal-occupancy is determined adaptively from the data, and can be anywhere and of any shape.

The procedure is flexible enough to admit a simple generalization to CFAR operation in the sense that, although a white background is assumed, its level may be unknown. There is little loss (less than 1 dB) from

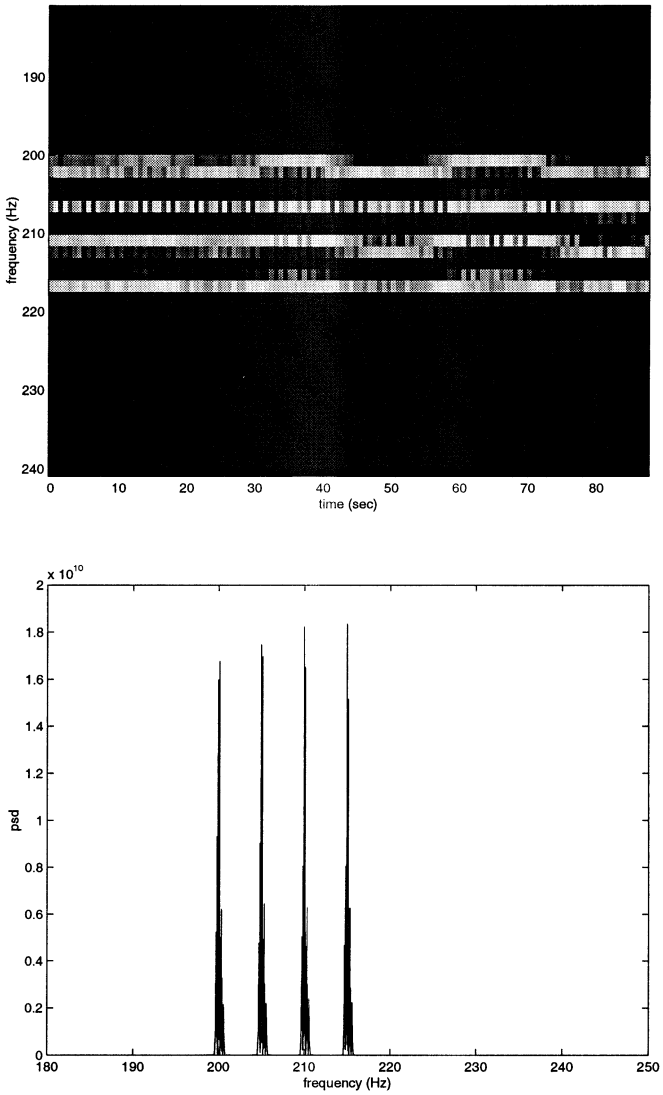

Fig. 12. Simulated signal with 4 coherently modulated tones in 200–220 Hz range. Aggregate SNR is here 70 dB, sampling frequency is 6 kHz, and frequency modulation is of low amplitude. Above: time-frequency plot. Below: magnitude-squared FFT of length 2^{19}. This is not the situation of interest in this paper, and the figure is for illustration only.

this generalization. A further generalization to the case that, due to multipath and relative Doppler shift or due to nonlinearity there may be multiple bands of signal energy, is also explored. It is discovered that not only is the procedure straightforward and numerically light, but also that there is little loss in overestimating the number of bands.

Adequate prewhitening of the signal is not always available, and hence we additionally present a version of the detector that performs self-normalization on a frequency-by-frequency basis. (It naturally requires a stationary background noise process in order to do this.) Much of the procedure in this case is identical to that in the previous cases; the exception is the formation of the GLR statistic itself, for which an alternative nonlinearity must be used. The performance of this new scheme is, as above, remarkably good, and this may be considered a "plug-in" solution for the detection of band-constrained signals.

APPENDIX A. COMPARISON OF TONE-CLUSTER AND NARROWBAND PROCESS MODELS

In the introductory section the uncertainty as to the model of the signal (harmonic set or narrowband process) was mentioned. This sounds uncomfortably vague, but it may genuinely be unknown what the nature of these signals is, and indeed whether their provenance is knowable at all. This is illustrated in the following figures. In Fig. 12 is shown the spectrum for a set of four coherently modulated tones in the range 200–220 Hz, shown for the space of between 1 and 2 min; the aggregate SNR (the overall signal energy divided by the per-sample noise variance) is an extremely high 70 dB. It is clear here that the

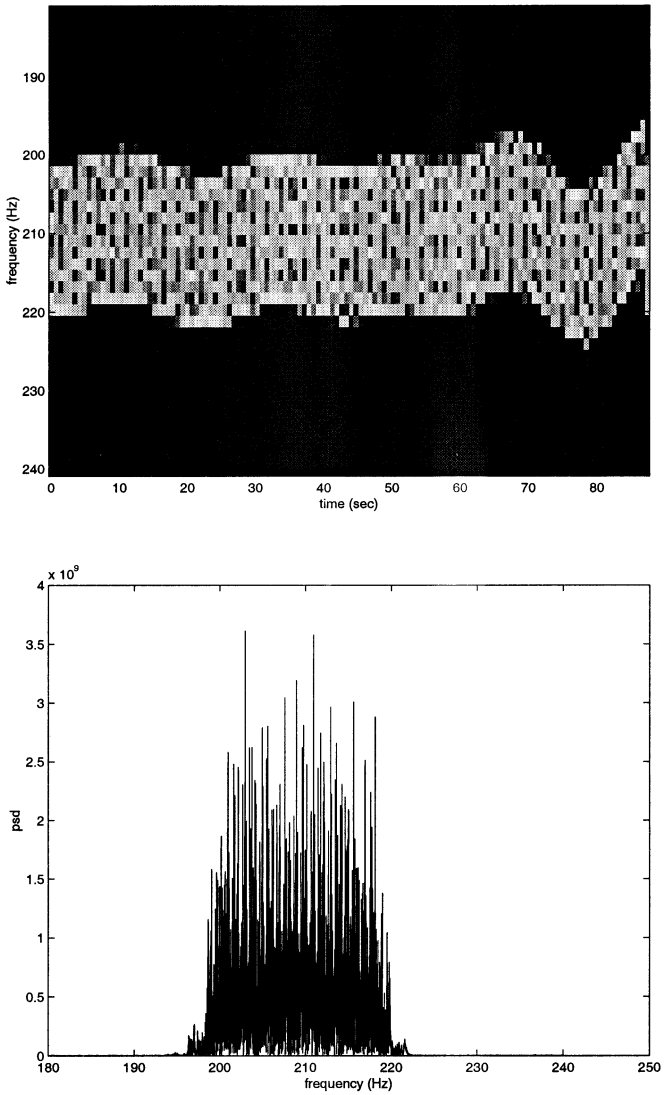

Fig. 13. Simulated signal with 10 coherently-modulated tones in 200–220 Hz range. Aggregate SNR is here 70 dB, sampling frequency is 6 kHz, and frequency modulation is of high amplitude. Above: time-frequency plot. Below: magnitude-squared FFT of length 2^{19}. This is not the situation of interest in this paper, and the figure is for illustration only.

signal is reasonably tonal, and that detection of such a signal should use this information. We contrast this with Fig. 13, in which the frequency modulation is higher amplitude than in the previous figure and in which there are now 10 modulated tones. From this it is observed that the "tonal" behavior of the signal is much less clear. The message from this figure is that whether or not the signal has tonal behavior may be moot. Figs. 12 and 13 are presented for illustration only. In Fig. 14 is shown an example of the signal with which this paper is concerned, with 100 tones, low modulation amplitude, and an aggregate SNR of 30 dB. Note that this corresponds to a sample-by-sample SNR of $1000 \times 2^{-19} = -27$ dB.

Let us assume that the harmonic-set model of (1) or (2) is true. To use this correctly, a GLR detector must contend with the performance loss due to imperfect (and sometimes catastrophic) estimation of the parameters. Still assuming the harmonic-set model, we contrast this with the situation that a GLR detector *designed* under model (3) is employed. There are now two sources of performance loss, that due to model mismatch, and that arising from imperfect estimation. Our contention is that one is better off to choose the second path, even though there are two sources of loss: it is evident that the second source of loss is smaller under assumption (3) than under an assumption of a harmonic set, and we contend that the first is relatively small given that the number of tones K is not small, and that due to the comparative paucity of the parameter set for estimation.

In fact, the immediate problem in demonstrating the claim is that parameter estimation is so difficult for a harmonic set. We thus simplify matters as much as possible, and consider the situation that the signal to be detected is a collection of

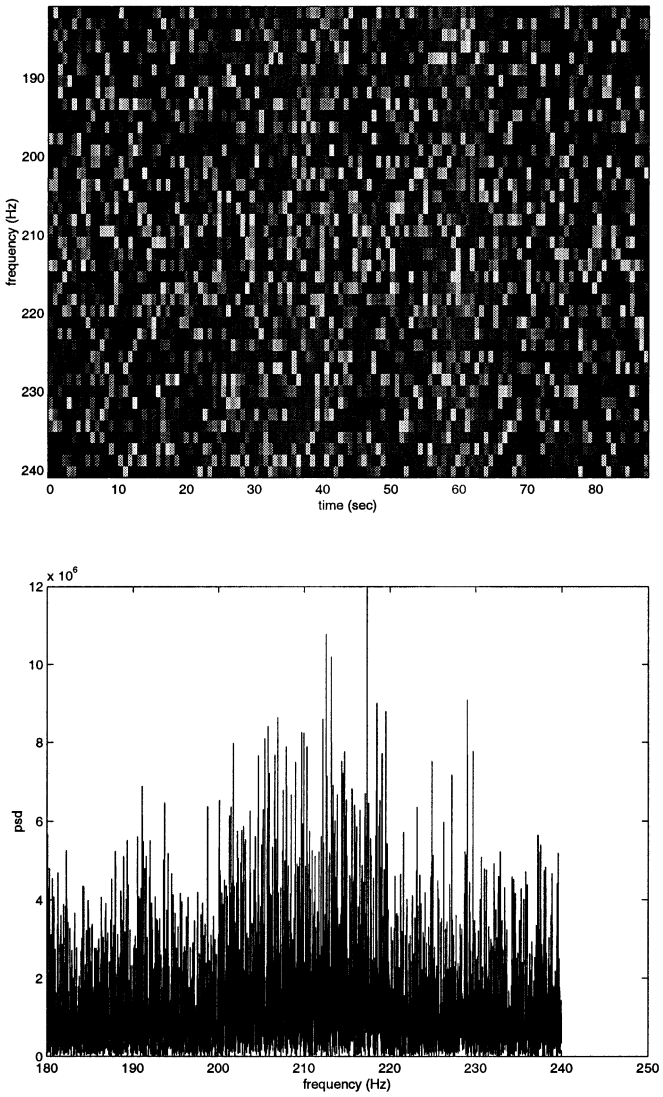

Fig. 14. Simulated signal with 100 coherently-modulated tones in 200–220 Hz range. Aggregate SNR is here 30 dB, sampling frequency is 6 kHz, and frequency modulation is of low amplitude. Above: time-frequency plot. Below: magnitude-squared FFT of length 2^{19}. This is the situation of interest in this paper.

K constant-frequency tones in a *known* frequency band—the tones are restricted to be within this band, but they are otherwise of unknown frequency. A Bayesian approach with a uniform prior distribution on the frequency-occupancy yields the approximately optimal[3] test statistics

$$T_{\text{Bayes}} = \sum_{\mathcal{S}} \exp\left(\sum_{k\in\mathcal{S}} X_k\right) \tag{38}$$

in which X_k denotes the magnitude-square of the kth DFT, and $\mathcal{S}$ is a set of K signal-occupying bins within the band of interest. The summation over the set $\mathcal{S}$ means that the summation is over all possible choices of K DFT bins in the band of interest; this detector is clearly infeasible. An alternative scheme is the GLRT, for which the test statistic is in this case simply

$$T_{\text{GLR}} = \sum_{k=1}^{K} X_{(k)} \tag{39}$$

in which $\{X_{(k)}\}$ is the descending-ordered population of DFT samples in the region of interest. This detector is feasible, but simulation has shown that it does not work particularly well when K is large.

Thus we invoke the work of Nuttall, who in [11] showed analytically that provided the exponent ν was suitably chosen (in the range $2 \le \nu \le 3$) there was little loss in using a power-law detector

$$T_{pl} = \sum_{k} X_k^{\nu} \tag{40}$$

[3]The "approximation" referred to is that the only possible frequencies are those which correspond to DFT bins.

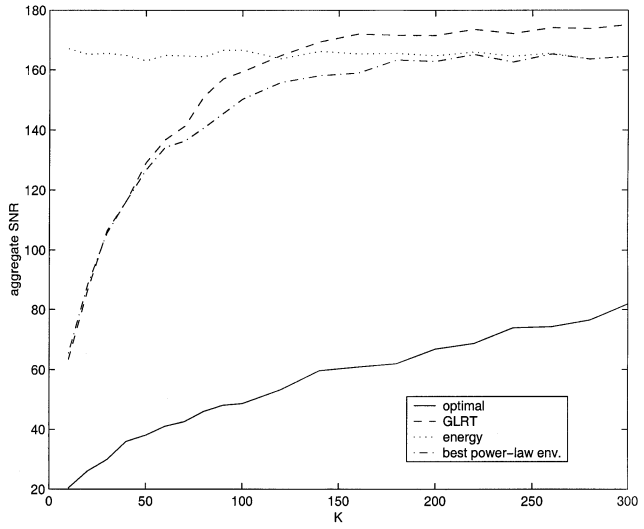

Fig. 15. Linear (nondecibel) plot of SNR necessary to achieve $P_{\rm d} = 70\%$ at $P_{\rm fa} = 0.01\%$ for various algorithms. Signal to be detected apportions its energy equally between K tones in a frequency band in which there are approximately 1365 DFT samples. The "optimal" scheme is clairvoyant, in that the locations of the tones are known to the detector. The "GLRT" scheme is $T_{\rm GLR}$ in (39), based on order statistics. The "energy" detector is that of (41), and the "best power-law" scheme is that based on (40). In this latter case, the best exponent ν varies with K; what is plotted is the best among all exponents (this decreases with K), and may be considered an envelope of performance.

as compared with the optimal detector (38).[4] We compare this to the detector

$$T_{nb} = \sum_k X_k \tag{41}$$

which *would* be optimal given that signal energy was equally apportioned between each DFT sample in the band of interest (note that in both (40) and (41) the summation is over all DFT samples in that band).

We simulate these in the following situation, with sampling rate 6 kHz, tone frequencies in the 20 Hz band [1200 Hz,1220 Hz], and signal duration of approximately 68 s. In Fig. 15 the aggregate SNR necessary to achieve probability of detection $P_{\rm d} = 70\%$ at operating false alarm rate $P_{\rm fa} = 10^{-4}$ is plotted against K, the number of frequency components. Note that the range of K shown is nontrivial, since with this length of data the approximate number of DFT bins in the 20 Hz band is approximately 1365. The conclusion from this figure is that the relative performance loss from use of (41) is relatively minor when the number of sinusoids K reaches 100. This was observed in [11]: an exponent $\nu = 1$, meaning the special case of (40) corresponding to (41), is close to optimal as the density of signal-containing DFT bins is no longer markedly sparse.

[4]In fact, although the range $2 \le \nu \le 3$ is good, there is some loss: a small ν is best for large K and a large ν for small K. In most simulations that follow we use the best ν for the situation at hand.

The signal of interest may arise from harmonic set model (1) or (2), or from narrowband process model (3). The form of the GLR statistic (5) does not depend on the complexity of the problem for estimation $\{\tilde{s}_n\}$; we have consequently examined a case in which estimation is far easier than for (1) or (2), that in which there is no frequency modulation. We have found that even here, there is little difference between the best available statistic using the correct model versus one using the mismatched model of (3). We conclude that it is acceptable to consider only detectors based on (3), and proceed next with the search for good means to estimate the band of occupancy.

APPENDIX B. DYNAMIC PROGRAMMING APPROACH TO FREQUENCY-DOMAIN SEGMENTATION

Let the frequency-domain data X, of size N, be composed of K segments with transition frequencies $\Omega = \{\omega_1, \omega_2, \ldots, \omega_{K-1}\}$. The data within segment k is characterized by the parameter μ_k, and therefore we write $\mu = \{\mu_1, \ldots, \mu_K\}$. For our observations X, defining $X[i,l] = \{X_{jm}, \text{for } i \le j \le l \text{ and } 1 \le m \le L\}$, we reformulate (8) into

$$f_\theta(\mathbf{X}) = \mathbf{f}(\mathbf{X}; \boldsymbol{\Omega}, \mu, \mathbf{K}) = \prod_{\mathbf{i=1}}^{\mathbf{K}} \mathbf{f}(\mathbf{X}[\boldsymbol{\omega}_{\mathbf{i-1}}, \boldsymbol{\omega}_{\mathbf{i}} - \mathbf{1}]; \mu_{\mathbf{i}}) \tag{42}$$

where $\omega_0 = 1$ and $\omega_K - 1 = N$ by definition, and $K = 3$, $\mu_1 = \mu_3 = 1$ and $\mu_2 >= 1$ in our problem. Defining

$$\begin{aligned} \Delta_i[\omega_{i-1}, \omega_i - 1] &= \ln f(X[\omega_{i-1}, \omega_i - 1]; \mu_i) \\ &= -L(\omega_i - \omega_{i-1}) \ln \mu_i - \frac{\sum_{m=1}^{L} \sum_{j=\omega_{i-1}}^{\omega_i - 1} X_{jm}}{\mu_i} \end{aligned} \tag{43}$$

where if μ_i is unknown, it should be replaced by its MLE

$$\mu_i = \mu_i^{\rm ML} = \frac{1}{L(\omega_i - \omega_{i-1})} \sum_{m=1}^{L} \sum_{j=\omega_{i-1}}^{\omega_i - 1} X_{jm}. \tag{44}$$

We wish to maximize $\sum_{i=1}^{K} \Delta_i[\omega_{i-1}, \omega_i - 1]$. Let

$$I_k(n) = \max_{\{\omega_1, \omega_2, \ldots, \omega_{k-1}\}, \omega_0 = 1, \omega_k = n+1} \sum_{i=1}^{k} \Delta_i[\omega_{i-1}, \omega_i - 1] \tag{45}$$

where $2 \le \omega_1 < \omega_2 < \cdots < \omega_{k-1} \le n$. Since

$$\begin{aligned} I_k(n) &= \max_{\omega_{k-1}, \omega_k = n+1} \max_{\{\omega_1, \omega_2, \ldots, \omega_{k-2}\}, \omega_0 = 1} \sum_{i=1}^{k} \Delta_i[\omega_{i-1}, \omega_i - 1] \\ &= \max_{\omega_{k-1}} [I_{k-1}(\omega_{k-1} - 1) + \Delta_k[\omega_{k-1}, n]]. \end{aligned} \tag{46}$$

The above maximization can be realized recursively, with only $\Delta_k[\omega_{k-1}, n]$ to be computed at each step. This is the DP formalism, and the computational complexity is significantly reduced as compared with a direct maximization. The solution to our original segmentation problem occurs for $k = K$ and $n = N$.

Assuming that there are exactly three segments (i.e., one spectral region of elevated energy), the GLRT based on DP is formulated as

$$T_{\mathrm{DP}} = I_3(N) - \ln f_{\theta_0}(\mathbf{X}) \tag{47}$$

where I_3 is from (46). If more than one signal band is allowed, the DP approach can be extended.

REFERENCES

[1] Baugh, K. (1992)
Parametric phase coupling in the vibration spectra of rolling element bearings.
Technical report, Applied Research Laboratory, University of Texas at Austin, 1992.

[2] Fawcett, J., and Maranda, B. (1991)
The optimal power law for the detection of a Gaussian burst in a background of Gaussian noise.
IEEE Transactions on Information Theory, **37**, 1 (1991), 209–214.

[3] Friedlander, B., and Porat, B. (1992)
Performance analysis of transient detectors based on a class of linear data transforms.
IEEE Transactions on Information Theory, **38**, 2 (1992), 665–673.

[4] James, B., Anderson, B., and Williamson, R. (1994)
Conditional mean and maximum likelihood approaches to multiharmonic frequency estimation.
IEEE Transactions on Signal Processing, (June 1994), 1366–1375.

[5] Johnson, N., Kotz, S., and Balakrishnan, N. (1995)
Continuous Univariate Distributions, Vol. 2 (2nd ed.).
New York: Wiley, 1995.

[6] Kay, S. (1998)
Fundamentals of Statistical Signal Processing: Vol. II: Detection Theory.
Englewood Cliffs, NJ: Prentice-Hall PTR, 1998, 200.

[7] Lehman, E. (1986)
Testing Statistical Hypotheses.
New York: Wiley, 1986.

[8] Luginbuhl, T., and Willett, P. (1999)
Tracking a general frequency modulated signal in noise.
In *Proceedings of the Conference on Decision and Control*, (Dec. 1999), 5076–5081.

[9] Nehorai, A., and Porat, B. (1986)
Adaptive comb filtering for harmonic signal enhancement.
IEEE Transactions on Signal Processing, (Oct. 1986), 1124–1138.

[10] Kenefic, R. (1998)
An algorithm to partition DFT data into sections of constant variance.
IEEE Transactions on Aerospace and Electronic Systems, **34**, 3 (1998), 789–795.

[11] Nuttall, A. (1994)
Detection performance of power-law processors for random signals of unknown location, structure, extent, and strength.
NUWC-NPT technical report 10,751, Sept. 1994.

[12] Nuttall, A. (1997)
Detection capacity of linear-and-power processor for random burst signals of unknown location.
NUWC-NPT technical report 10,822, Aug. 1997.

[13] Nuttall, A. (1995)
Near-Optimum detection of random signals of unknown location, structure, extent, and strength.
OCEANS '95. Conference Proceedings, MTS/IEEE. Challenges of Our Changing Global Environment, 3 (1995), 1659–1664.

[14] Parker, P., and Anderson, B. (1990)
Frequency tracking of nonsinusoidal signals in noise.
Signal Processing, **20** (1990), 127–152.

[15] Porat, B. (1997)
A Course in Digital Signal Processing.
New York: Wiley, 1997.

[16] Strang, G., and Nguyen, T. (1996)
Wavelet and Filter Banks.
Wellesley, MA: Wellesley-Cambridge Press, 1996.

[17] Streit, R., and Willett, P. (1999)
Detection of random transient signals via hyperparameter estimation.
IEEE Transactions on Signal Processing, (July 1999), 1823–1843.

[18] Wang, Z., and Willett, P. (2001)
All-purpose and plug-in power-law detectors for transient signals.
IEEE Transactions on Signal Processing, (Nov. 2001), 2454–2466.

[19] Wang, Z., and Willett, P. (2000)
A performance study of some transient detectors.
IEEE Transactions on Signal Processing, (Sept. 2000), 2682–2685.

[20] White, L. (1993)
An iterative method for exact maximum likelihood estimation of the parameters of a harmonic series.
IEEE Transactions on Automatic Control, (Feb. 1993), 367–370.

[21] Zhou, G., and Giannakis, G. (1995)
Retrieval of self-coupled harmonics.
IEEE Transactions on Signal Processing, (May 1995), 1173–1186.

[22] So, H., Chan, Y., Ma, O., and Ching, P. (1999)
Comparison of various periodograms for sinusoid detection and frequency estimation.
IEEE Transactions on Aerospace and Electronic Systems, **35**, 3 (July 1999), 945–950.

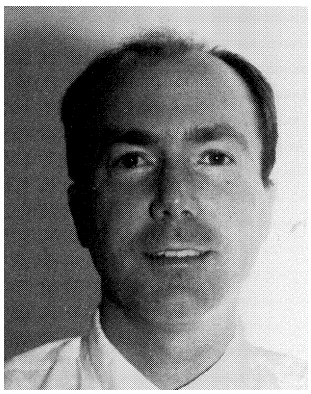

Peter K. Willett (S'83—M'86—SM'97) was born in Toronto, Ont., Canada. He received the B.Sc. degree in engineering science from the University of Toronto in 1982. He received the M.E. and M.S. degrees in 1983 and 1984, respectively, and the Ph.D. degree in 1986, all in electrical engineering, from Princeton University, Princeton, NJ.

He is professor with the University of Connecticut, Storrs, where he has been since 1986. His interests are generally in detection theory, target tracking, and signal processing.

Dr. Willett is an Associate Editor for the *IEEE Transactions on Sytems, Man, and Cybernetics* and the *IEEE Transactions on Aerospace and Electronic Systems*.

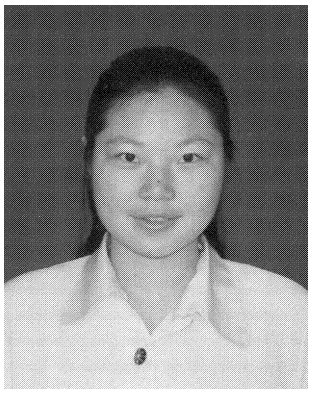

Zhen Wang was born in China in 1974. She received the B.Sc. degree (honors) from Tsinghua University, Beijing, China, in 1996, and the M.Sc. degree from the University of Connecticut, Storrs, in 2000, both in electrical engineering.

She is currently working towards the Ph. D. degree at the University of Connecticut. Her present research interests include detection theory, communications and signal processing.

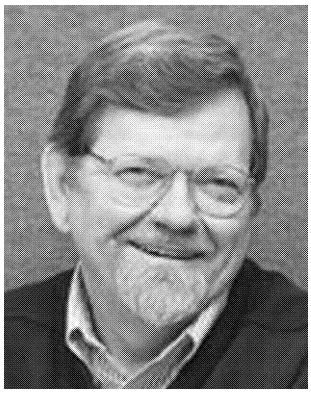

Roy L. Streit received the Ph.D. in mathematics from the University of Rhode Island, Kingston, in 1978.

He has been with the Naval Undersea Warfare Center since 1970, when he joined one of its predecessor organizations, the Navy Underwater Sound Laboratory in New London, CT. From 1981–1982, he was a Visiting Scholar with the Department of Operations Research, Stanford University. From 1982 to 1984, he was a Visiting Scientist with the Computer Science Department, Yale University. From 1987 to 1989, he was an Exchange Scientist with the Defence Science and Technology Organization in Adelaide, Australia. His current research interests include passive detection and localization of distributed targets in hyperspectral images, tracking in random media using low fidelity environmental wave propagation models, and numerical acoustic hull array design. He is currently a Senior Technologist for Acoustic Signal Processing.

Dr. Streit received the 1999 Solberg Award from the American Society of Naval Engineers for outstanding achievement in research and development related to naval engineering.